Microarray Analysis of XOPS-mCFP Zebrafish Retina Identifies Genes Associated with Rod Photoreceptor Degeneration and Regeneration

Ann C. Morris,[1] *Marie A. Forbes-Osborne,*[1] *Lakshmi S. Pillai,*[1] *and James M. Fadool*[2]

Purpose. XOPS-mCFP transgenic zebrafish experience a continual cycle of rod photoreceptor development and degeneration throughout life, making them a useful model for investigating the molecular determinants of rod photoreceptor regeneration. The purpose of this study was to compare the gene expression profiles of wild-type and XOPS-mCFP retinas and identify genes that may contribute to the regeneration of the rods.

Methods. Adult wild-type and XOPS-mCFP retinal mRNA was subjected to microarray analysis. Pathway analysis was used to identify biologically relevant processes that were significantly represented in the dataset. Expression changes were verified by RT-PCR. Selected genes were further examined during retinal development and in adult retinas by in situ hybridization and immunohistochemistry and in a transgenic fluorescent reporter line.

Results. More than 600 genes displayed significant expression changes in XOPS-mCFP retinas compared with expression in wild-type controls. Many of the downregulated genes were associated with phototransduction, whereas upregulated genes were associated with several biological functions, including cell cycle, DNA replication and repair, and cell development and death. RT-PCR analysis of a subset of these genes confirmed the microarray results. Three transcription factors (*sox11b*, *insm1a*, and c-*myb*), displaying increased expression in XOPS-mCFP retinas, were also expressed throughout retinal development and in the persistently neurogenic ciliary marginal zone.

Conclusions. This study identified numerous gene expression changes in response to rod degeneration in zebrafish and further suggests a role for the transcriptional regulators *sox11b*, *insm1a*, and c-*myb* in both retinal development and rod photoreceptor regeneration. (*Invest Ophthalmol Vis Sci.* 2011;52:2255–2266) DOI:10.1167/iovs.10-6022

Photoreceptors are specialized sensory neurons in the retina that transduce the energy from photons of light into electrical signals. Rod photoreceptors mediate visual responses in dim light, whereas cone photoreceptors mediate daytime and color vision. Mutations in several genes cause retinopathic diseases such as retinitis pigmentosa (RP), a genetically inherited blinding disorder characterized by progressive degeneration of the rod photoreceptors and secondary degeneration of the cones (RetNet: http://www.sph.uth.tmc.edu/Retnet/). To develop effective treatments for diseases such as RP and to better understand its pathogenesis, we need a thorough understanding of the molecular mechanisms that regulate rod photoreceptor genesis. Although some key molecules have been identified, the transcriptional regulatory network regulating rod photoreceptor development remains to be fully defined.

The zebrafish is an excellent genetic model organism in which to study the mechanisms of rod photoreceptor determination.[1] The zebrafish retina possesses the same laminar organization and cell types found in higher vertebrates.[2] Zebrafish embryos develop externally, and both embryos and newly hatched larvae are optically transparent, greatly facilitating the study of developmental processes and gene expression during retinogenesis. Furthermore, development is extremely rapid; by 3 days after fertilization (dpf) the zebrafish retina is fully laminated, and by 5 dpf zebrafish larvae are actively swimming and demonstrate visually evoked behavior.[3,4] Finally, zebrafish (like other teleost fish) demonstrate persistent retinal neurogenesis throughout life and are able to regenerate all retinal cell types in response to acute injury.[5]

Studies of retinal regeneration in zebrafish are particularly relevant, because cell-based treatments for retinal degenerative diseases must enable photoreceptor replacement in the context of a fully mature tissue, and this is likely to involve overlapping yet distinct regulatory pathways from those used during embryonic photoreceptor development. To better understand the molecular mechanisms that mediate photoreceptor regeneration in zebrafish, our laboratory has focused on characterizing genetic models of selective photoreceptor loss and replacement. One such model is the XOPS-mCFP transgenic line, in which the toxic effect of a rod-targeted fluorescent reporter gene causes selective degeneration of rods.[6]

We have shown previously that the rod photoreceptor degeneration caused by the XOPS-mCFP transgene does not result in secondary degeneration of cones. Furthermore, in contrast to what has been observed after acute retinal injury or large-scale ablation of the rods in zebrafish, chronic, progressive rod photoreceptor loss in XOPS-mCFP retinas does not induce proliferation of retinal Müller glia.[6] Rather, a population of rod progenitor cells located in the outer nuclear layer (ONL) increases proliferation in an attempt to regenerate the lost rods. In the healthy adult retina, rod progenitor cells produce new rods at a slow but steady rate.[2,7] However, in XOPS-mCFP zebrafish the rod progenitor population is increased several fold, suggesting that this pool of committed progenitor cells mediates regeneration in cases of chronic rod loss.[6]

The specific amplification of the rod progenitor population in XOPS-mCFP retinas provides a unique opportunity to study the molecular determinants of rod photoreceptor development

From the [1]Department of Biology, University of Kentucky, Lexington, Kentucky; and the [2]Department of Biological Science and Program in Neuroscience, Florida State University, Tallahassee, Florida.

Supported by NIH Grant R01 EY017753.

Submitted for publication June 9, 2010; revised August 29, 2010; accepted November 3, 2010.

Disclosure: **A.C. Morris**, None; **M.A. Forbes-Osborne**, None; **L.S. Pillai**, None; **J.M. Fadool**, None

Corresponding author: Ann C. Morris, 215 T. H. Morgan Building, Department of Biology, University of Kentucky, Lexington, KY 40506-0225; ann.morris@uky.edu.

in adult zebrafish in greater detail. We therefore performed a microarray analysis of retinal RNA from wild-type and XOPS-mCFP adults. Several genes displaying increased expression in response to rod photoreceptor degeneration were identified, including many transcription factors with previously uncharacterized roles in the retina. RT-PCR and in situ hybridization verified the microarray results and also suggested a role for some of these genes during retinal development and regeneration.

METHODS

Wild-Type and Transgenic Zebrafish

Rearing, breeding, and staging of zebrafish were performed in accordance with established methods for zebrafish animal husbandry.[8] Wild-type zebrafish were inbred descendants of the Ekwill strain, originally obtained from the Ekkwill fish farm (Gibsonton, FL). The Tg(XRho:gap43-mCFP)q13 transgenic line, referred to herein as XOPS-mCFP, has been described previously.[6,9] It harbors a fluorescent mCFP reporter transgene under the control of the *Xenopus* rhodopsin promoter, the expression of which is toxic to the rod photoreceptors. The *c-myb-GFP* transgenic line has also been described,[10,11] and was generously provided by Leonard Zon (Harvard Medical School, Boston, MA). All animals were treated in accordance with the ARVO Statement for the Use of Animals in Ophthalmic and Vision Research.

RNA Preparation

For the microarray analysis, four wild-type and four XOPS-mCFP adults (10–11 months of age) were killed by immersion in MS-222 (Tricaine; Sigma-Aldrich, St. Louis, MO). The right eye was dissected, and the sclera, choroid and lens were removed. The retinas were transferred to microcentrifuge tubes containing RNA stabilizer (RNA later; Ambion/Applied Biosystems, Austin, TX). Individual retinas were not pooled. Total RNA was prepared from each sample (RNeasy kit; Qiagen, Valencia, CA) according to the manufacturer's instructions.

Microarray Analysis

RNA samples were submitted to the Gene Expression Core Facility at the University of Florida's Interdisciplinary Center for Biotechnology Research (ICBR; Gainesville, FL). RNA quality and concentration were assessed with a bioanalyzer (model 2100; Agilent Technologies, Palo Alto, CA). Preparation of cDNA, generation and fluorescent labeling of cRNA, and chip hybridization were performed by the ICBR, according to standard protocols. Fluorescently labeled wild-type and XOPS-mCFP cRNAs were co-hybridized to a zebrafish microarray containing 42,990 probes representing roughly 21,500 zebrafish ESTs (4 × 44k; Agilent Technologies). Eight hybridizations (representing four individual wild-type and XOPS-mCFP retinas) were performed. The hybridizations included a reciprocal dye-swap control to account for biological, sample preparation, and technical variability. Microarray scanning and image processing were performed by the ICBR (Feature Extraction software; Agilent Technology). The intensity of each spot was summarized by the mean pixel intensity. After background subtraction, raw data were normalized by Lowess transformation. A two-way ANOVA comparison was used for differential expression analysis (Analyze-It, Excel; Microsoft, Redmond, WA). The *P*-values were adjusted using the Benjamini and Hochberg[12] method to control for false discovery rate. Differentially expressed genes were ranked by the adjusted *P*-values; genes with a $P < 0.005$ were considered to be differentially expressed between wild-type and XOPS-mCFP retinas. The data discussed in this report have been deposited in the National Center for Biotechnology Information (NCBI; Bethesda, MD) Gene Expression Omnibus (GEO)[13] and are accessible through GEO Series Accession Number GSE22221 (http://www.ncbi.nlm.nih.gov/geo/query/acc.cgi?acc=GSE22221).

Gene Ontology and Pathway Analysis

Genes displaying an absolute change of twofold or greater were uploaded to the GFinder (Genome Function Integrated Discoverer; Bio-Medical Informatics Laboratory, Politecnico di Milano, Milan, Italy) database[14] for initial functional annotation and classification based on gene ontology assignment (http://www.medinfopoli.polimi.it/GFINDer/). The differentially expressed gene list was next subjected to pathway analysis to identify biologically relevant processes that were most significantly represented in the dataset. After removal of unannotated entries, the list of differentially expressed genes and corresponding $\log_2$ change ratios were uploaded into a pathway analysis program (IPA; Ingenuity Systems, Redwood, CA). IPA maintains a manually curated knowledge base containing information on human, mouse, and rat gene function and biological interactions drawn from the scientific literature. The zebrafish genes in the differentially expressed dataset were assigned to a corresponding human, mouse, or rat identifier in the IPA Knowledge Base using the NCBI HomoloGene database. The IPA Functional Analysis tool was used to identify biological functions that were significantly associated with the genes in the dataset. The IPA program uses a right-tailed Fisher's exact test to calculate a *P*-value associated with the probability that each biological function was identified due to chance alone. To determine whether any canonical pathways are significantly associated with the dataset, the IPA software calculates a ratio of the number of molecules from the dataset that are associated with a given canonical pathway divided by the total number of molecules that map to that pathway; a Fisher's exact test was used to calculate a *P*-value representing the probability that the association between the genes in the dataset and the canonical pathway is by chance alone.

Reverse Transcription-Polymerase Chain Reaction

Eyes were dissected from wild-type and XOPS-mCFP transgenic adults as described earlier. The retinas from two to four adults were pooled to purify RNA for RT-PCR. Total RNA was prepared from dissected retinas (Trizol reagent; Invitrogen, Carlsbad, CA). Approximately 1 μg of RNA was reverse transcribed into cDNA (Superscript III Reverse Transcriptase; Invitrogen). The sequences of the PCR primers used in this study are given in Table 1.

In Situ Hybridization

In situ hybridization of embryonic, larval, and adult retinal cryosections was performed essentially as previously described.[9] PCR products corresponding to the genes of interest were amplified from retinal or embryonic cDNA and cloned into a vector (pGemT-Easy; Promega, Madison, WI). Digoxigenin (DIG)- or fluorescein (Fluor)-labeled antisense and sense riboprobes were prepared by in vitro transcription with T7 or SP6 polymerase using the an RNA labeling kit (Roche Applied Science, Indianapolis, IN) according to the manufacturer's instructions. Cryosections (10–14-μm-thick) were prepared from tissue that had been fixed overnight in 4% paraformaldehyde and subsequently cryoprotected in 30% sucrose. Tissue was embedded in OCT medium (Miles Scientific, Elkhart, IN), and cryosections were mounted (Superfrost Plus slides; Fisher Scientific, Pittsburgh, PA) and air dried overnight. Riboprobes were hybridized to the sections overnight at 58°C to 65°C at a final concentration of 1 to 3 ng/μL The sections were washed and incubated with anti-DIG-AP or anti-Fluor-AP (Roche) overnight at 4°C. They were then incubated in coloration buffer containing NBT and BCIP (Roche) or Fast Red (Sigma-Aldrich) for 4 hours at room temperature or 1 to 2 days at 4°C and imaged with bright field optics on an inverted fluorescence microscope (Eclipse Ti-U; Nikon), using a 40× air objective.

Immunohistochemistry

Immunolabeling of larval and adult cryosections was performed as previously described.[6] Images were obtained with one of two microscopes (Axiovert fluorescence microscope or a model 510 confocal microscope; both from Carl Zeiss Meditec) outfitted with a 40× water

TABLE 1. PCR Primers

Gene	NCBI Accession Number	Forward Primer (5′–3′)	Reverse Primer (5′–3′)	Amplicon (bp)
atp5b	NM_200702	TGCCATCTCAGCAAAACTTG	CACAGGCTCAGGAACAGTCA	142
bmp4	NM_131342	GACCCGTTTTACCGTCTTCA	TTTGTCGAGAGGTGATGCAG	142
c-myb	NM_131266	CTCTACCTTCCTCTCGAACAGC	GTCTTTGGTTCCTTGAATGATGGC	2008, 2160
dnmt1	NM_131189	TTCAACTCGCGCACATACTC	CAGTGTGAGCTTCAGGACCA	150
elov4	NM_199972	CACGTCTCAAGACAGCCAAA	TCTTTCCATTTTCCGTGACC	90
fzd10	NM_130917	CTCGACAAACAATGGGTGTG	GCCAAAGCCTTATTGAGCAG	141
gc1	AY050503	TCACCACAGGGAGTTTCCTC	TTGGGTGATTTCTGGGTCTC	128
hdac9b	NM_200816	CGCTGCCCAATATCTCTCTC	GTATGCGCATCTGCGTTCTA	143
her12	NM_205619	AGGCTGACATCCTGGAAATG	GCGAGAGGAAGTGGACAGAC	129
id2b	NM_199541	GCCCCAATTCACTTAGAAAG	GGACTTTTAACCAAACAAGCG	252
insm1a	NM_205644	GGCACCACAGTAACCACCA	CGCTGGAAGTCTCCTCTTTCT	421
insm1b	NM_199658	GTTGATGTACCTCTGCCTTGAA	GTGACACAGGGGAGAAAAGTC	
notch1a	NM_131441	GCATCTCAGCCGTGTCTCAACG	TAATACGACTCACTATAGGGTTGC TGGAGCACTCGTTGTGC	384
notch3	NM_131549	TACTGTGCTGAGGATGTCAACG	TAATACGACTCACTATAGGTTAGGTC GGTCAATGCACTTGG	
nr1d1	NM_205729	GTGAACAACCAGCTGCAGAA	ACTGTAAGGCCTGGACATGG	125
sox11a	NM_131336	ATTTCTTTCCCCTGCCTTCCACTG	TATTTTCACTACCGATTGTTCTTT	360
sox11b	NM_131337	GCTGGCACATTCTCCAATTT	TTGCTACAAAACGCAGATGG	1050
stat3	AB018219	CCCCGTGTCCTTCTGTCTTC	GGCTTCGTTGTGCATGAGAGAG	139
wnt2	NM_130950	AAACTGGATTGGCGAATGTC	ACAAAAGCTGCCTCACGACT	123

immersion objective (NA 1.2 C-Apochromat; Carl Zeiss Meditec). The following primary antibodies were used: anti-GFP (rabbit, 1:1000; Ab-Cam, Cambridge UK); and Zrf-1, which labels Müller glia (mouse, 1:10; Oregon Monoclonal Bank, Eugene, OR). Alexa Fluor–conjugated secondary antibodies (Molecular Probes-Invitrogen, Eugene, OR) were all used at a dilution of 1:200. Sections were counterstained with DAPI (4′, 6-amidino-2-phenylindole, 1:10,000; Sigma) to visualize cell nuclei. The images were exported to imaging software for figure preparation (Photoshop; Adobe Systems, Mountain View, CA).

RESULTS

Microarray Analysis of Wild-Type and XOPS-mCFP Retinas

To identify gene expression changes associated with the degeneration and regeneration of rod photoreceptors, retinal mRNA was prepared from four individual wild-type, age-matched XOPS-mCFP adult zebrafish at approximately 1 year of age. Fluorescently labeled cRNA was prepared from each mRNA sample by the Gene Expression Core Facility of the Interdisciplinary Center for Biotechnology Research (ICBR) at the University of Florida. The cRNA was hybridized to a zebrafish gene expression chip (Agilent Technologies) containing probes for 21,500 zebrafish transcripts. Each of the four replicate hybridizations included a dye-swap control. Preliminary data analysis, including signal extraction, background subtraction, Lowess transformation, and a two-way ANOVA comparison, was performed by the ICBR.

Using this approach, 680 transcripts displaying absolute expression changes of greater than twofold in XOPS-mCFP retinas compared with wild-type controls were identified. The top 30 upregulated and downregulated transcripts in XOPS-mCFP retinas are listed in Tables 2 and 3, respectively (only annotated transcripts are listed). In cases where probes for the indicated genes were spotted in duplicate on the microarray, only one probe ID is given, and the corresponding change ratio shown is the average of both results. A comprehensive list of all transcripts displaying significant changes in expression between XOPS-mCFP and wild-type retinas is available from the NCBI Gene Expression Omnibus (GEO) website (accession number: GSE22221). Approximately 87% of the genes showed an increase in expression in XOPS-mCFP retinas relative to wild-type, whereas the remaining 13% displayed decreased expression in XOPS-mCFP retinas. The maximum $\log_2$ change ratios were 7.32 and −6.82, respectively.

Ontology and Pathway Analysis of Gene Expression Dataset

An initial analysis of the microarray gene expression data was performed by using GFINDer (http://www.medinfopoli.polimi.it/GFINDer/). Genes displaying an absolute change ratio of 2 or greater were uploaded to the GFINDer database, where they were grouped according to their annotation in The Gene Ontology database. One of the largest groups of genes to emerge from this analysis contained gene ontology assignments related to cell proliferation, such as cell cycle, DNA replication, and mitosis. The genes in this group are shown in Supplementary Table S1 (http://www.iovs.org/lookup/suppl/doi:10.1167/iovs.10-6022/-/DCSupplemental), along with their Agilent Probe IDs and change in expression in XOPS-mCFP retinas compared with wild-type. Another large group of genes that displayed significant expression changes are transcriptional regulators. These genes are listed in Supplementary Table S2 (http://www.iovs.org/lookup/suppl/doi:10.1167/iovs.10-6022/-/DCSupplemental). Genes corresponding to the functional category of signal transduction are shown in Supplementary Table S3 (http://www.iovs.org/lookup/suppl/doi:10.1167/iovs.10-6022/-/DCSupplemental), whereas genes related to apoptosis are shown in Supplementary Table S4 (http://www.iovs.org/lookup/suppl/doi:10.1167/iovs.10-6022/-/DCSupplemental).

To gain further insight into the biological significance of the gene expression changes observed by microarray analysis, the set of annotated genes displaying a change of 2 or greater was submitted to pathway analysis (Pathway Analysis database; Ingenuity). For the analysis, the zebrafish genes were first assigned to a human, mouse, or rat homologue using the NCBI HomoloGene database. Of the 464 annotated genes that were uploaded to the IPA database, 324 received unambiguous assignment to a corresponding human, mouse, or rat homologue and were further analyzed by the IPA program.

The IPA program identifies gene networks associated with known biological pathways that demonstrate a statisti-

TABLE 2. Top 30 Upregulated Genes in XOPS-mCFP Retinas Compared with Wild-Type

Agilent Probe ID	Gene Symbol	Gene Name	Log^2 Fold-Change	*P*-value
A_15_P109009	*mhcluba*	Major histocompatibility complex class I UBA	7.32	0.00796
A_15_P118874	*mhc1uea*	Major histocompatibility complex class I UEA gene	7.09	2.9862^{-12}
A_15_P116359	*ndufv1*	NADH dehydrogenase (ubiquinone) flavoprotein 1	6.32	4.5000^{-12}
A_15_P120879	*psmb9a*	Proteasome (prosome, macropain) subunit, beta type, 9a	5.20	5.5938^{-13}
A_15_P112031	*foxk1*	Forkhead box K1	4.54	2.8185^{-07}
A_15_P109699	*dlgap5*	Discs, large (*Drosophila*) homolog-associated protein 5	4.13	1.4218^{-10}
A_15_P118880	*kifl1*	Kinesin family member 11	4.03	3.665^{-11}
A_15_P116883	*dlb*	DeltaB	4.03	1.9109^{-09}
A_15_P103535	*c-myb*	Transcription factor c-myb	4.00	2.0605^{-10}
A_15_P120882	*glrx*	Glutaredoxin (thioltransferase)	3.94	4.0637^{-12}
A_15_P120727	*mcm5*	Minichromosome maintenance deficient 5 (*S. cerevisiae*)	3.90	8.8000^{-10}
A_15_P100423	*tdc2*	Cell division cycle 2	3.89	4.1462^{-11}
A_15_P106119	*tph2*	Tryptophan hydroxylase 2 (tryptophan 5-monooxygenase)	3.79	9.6829^{-07}
A_15_P100081	*gsnl1*	Gelsolin, like 1	3.66	0.00376
A_15_P105192	*rrm2*	Ribonucleotide reductase M2 polypeptide	3.65	0.00032
A_15_P119814	*tyms*	Thymidylate synthase	3.63	1.3629^{-10}
A_15_P106314	*trip13*	Thyroid hormone receptor interactor 13	3.50	1.1598^{-09}
A_15_P110081	*foxm11*	Forkhead box M1-like	3.49	1.2704^{-11}
A_15_P100639	*asf1b*	Anti-silencing function 1 homolog B (*S. cerevisiae*)	3.36	2.7872^{-09}
A_15_P101975	*wdr51b*	WD repeat domain 51B	3.34	8.9146^{-11}
A_15_P103981	*kifc1*	Kinesin family member C1	3.33	1.2032^{-09}
A_15_P120024	*hnrpa0*	Heterogeneous nuclear ribonucleoprotein A0	3.28	6.1726^{-10}
A_15_P101117	*depdc1a*	DEP domain containing 1a	3.26	3.6250^{-11}
A_15_P103444	*mcm4*	Minichromosome maintenance deficient 4 (*S. cerevisiae*)	3.24	3.8500^{-11}
A_15_P109617	*ccnb2*	Cyclin B2	3.23	1.7127^{-08}
A_15_P116200	*g2e3*	G2/M-phase specific E3 ubiquitin ligase	3.23	6.4917^{-09}
A_15_P104699	*ncapd3*	Non-SMC condensia II complex, subunit D3	3.22	2.1112^{-09}
A_15_P116547	*mthfd2*	Methylenetetrahydrofolate dehydrogenase (NADP+ dependent) 2	3.16	6.1977^{-06}
A_15_P110975	*nstm*	Nucleostemin	3.15	1.7644^{-05}
A_15_P101762	*dtl*	Denticleless homolog (*Drosophila*)	3.08	1.3481^{-09}

cally significant association with genes in the microarray data set. The top 10 functional networks identified by the IPA program are graphed in Figure 1A. These include biological functions associated with the cell cycle, cell death, cellular development, and DNA replication, recombination and repair. Figure 1B shows the top 10 canonical pathways demonstrating a significant association with groups of genes in the microarray dataset. The IPA canonical pathways database contains well characterized metabolic and cell signaling pathways that are manually curated based on information from published scientific literature, review articles, text books, and the KEGG database.

The top three canonical pathways displaying significant association with genes in the microarray dataset are diagrammed in Figure 2. The filled-in symbols correspond to genes that were differentially expressed between wild-type and XOPS-mCFP retinas, with green or red shading, indicating increased or decreased expression in XOPS-mCFP retina, respectively. Figure 2A illustrates the ATM signaling pathway, which is induced by DNA damage and activates several downstream pathways, including DNA repair, cell cycle checkpoints, apoptosis, and cell cycle arrest or progression. Genes contributing to this pathway displayed increased expression in XOPS-mCFP retinas, and include the Chk1 and Chk2 checkpoint kinases, cyclins and cyclin dependent kinases associated with progression of S and G_2/M phases, the growth arrest factor GADD45γ, H2AX, a histone associated with DNA damage, the cohesin factor SMC, IκBα, a regulator of NF-κB signaling, and the transcription factor c-Jun. Expression of the ATM gene itself increased 1.89-fold in XOPS-mCFP retinas compared to wild-type, below the twofold cutoff for inclusion in the IPA dataset, but statistically significant across all replicates. It is therefore represented with hatched shading in Figure 2A to indicate its manual annotation in the pathway. Figure 2B illustrates pathways associated with the mitotic roles of the polo-like kinase (PLK). Again, the differentially expressed genes associated with this canonical pathway all displayed increased expression in XOPS-mCFP retinas and include the cell cycle genes mentioned above, as well as CDC20 and CDC7, the cytokinesis regulator PRC1, and the kinesins EG5/KIF11 and MKLP1. Figure 2C illustrates the rod phototransduction pathway. All but one of the differentially expressed genes associated with this pathway displayed a decrease in expression in XOPS-mCFP retinas. Because mature rod photoreceptors degenerate in XOPS-mCFP animals, the identification of these genes in our microarray analysis served as an important internal control. A probe for the rhodopsin gene was not present on the version of the Agilent microarray that was used for these experiments. However, our previous work has clearly demonstrated a reduction in rhodopsin expression in XOPS-mCFP retinas due to the degeneration of the rods[6,9]; it is therefore manually annotated on the pathway with hatched shading.

Validation of Microarray Data by RT-PCR

To confirm the microarray results, RT-PCR of wild-type and XOPS-mCFP retinal mRNA was performed for a subset of the genes displaying significant expression changes (Fig. 3). The cDNA for all PCR analyses was prepared from separate groups of animals from those used for the microarray analysis. Although the RT-PCR results are not quantitative, every gene that was tested confirmed the general change in expression (increased, decreased or no change) between wild-type and XOPS-mCFP retinas, as indicated by the microarray results.

TABLE 3. Top 30 Downregulated Genes in XOPS-mCFP Retimas Compared with Wild-Type

Agilent Probe ID	Gene Symbol	Gene Name	Log^2 Fold-Change	*P*-value
A_15_P118676	*pde6a*	Phosphodiesterase 6A, cGMP-specific, rod, alpha	−6.82	2.6250^{-13}
A_15_P101838	*guca1b*	Guanylate cyclase activator 1B	−5.76	4.9500^{-14}
A_15_P113186	*id21*	Inhibitor of DNA binding 2, dominant negative helix-loop-helix protein, like	−4.87	4.0500^{-12}
A_15_P102352	*efr3a*	EFR3 homolog A (*S. cerevisiae*)	−4.58	9.4220^{-11}
A_15_P114606	*gc2*	Guanylyl cyclase 2	−4.56	2.2358^{-11}
A_15_P121315	*mpzl3*	Myelin protein zero-like 3	−4.56	3.5362^{-10}
A_15_P115098	*pdc1*	Phosducin 1	−4.43	6.4092^{-13}
A_15_P119137	*aanat1*	Arylalkylamine N-acetyltransferase 1	−4.40	2.6440^{-13}
A_15_P109931	*gucy2f*	Guanylate cyclase 2F, retinal	−4.21	9.0294^{-07}
A_15_P110628	*gng1*	Guanine nucleotide binding protein (G protein), gamma 1 subunit	−4.17	4.5542^{-11}
A_15_P103716	*gucala*	Guanylate cyclase activator 1A	−4.16	8.9500^{-10}
A_15_P101719	*pdyn*	Prodynorphin	−3.56	3.9442^{-13}
A_15_P112352	*tmem136*	Transmembrane protein 136	−3.16	3.2926^{-08}
A_15_P109812	*rgs9bp*	Regulator of G-protein signalling 9 binding protein	−3.02	6.1639^{-06}
A_15_P109394	*vps36*	Vacuolar protein sorting 36 homolog (*S. cerevisiae*)	−2.82	9.7379^{-11}
A_15_P101327	*gnb1*	Guanine nucleotide binding protein (G protein), beta polypeptide 1	−2.58	3.6756^{-10}
A_15_P120462	*rhpn2*	Rhophilin, Rho GTPase binding protein 2	−2.54	3.3963^{-07}
A_15_P116591	*elovl4*	Elongation of very long chain fatty acids-like 4	−2.53	2.1284^{-08}
A_15_P108954	*pde6g*	Phosphodiesterase 6G, cGMP-specific, rod, gamma	−2.20	4.8961^{-10}
A_15_P113348	*mbn12*	Muscleblind-like 2 (*Drosophila*)	−2.02	4.4048^{-09}
A_15_P117184	*krill*	KRI1 homolog like	−1.90	1.5549^{-08}
A_15_P106511	*nipa1*	Non imprinted in Prader-Willi/Angelman syndrome 1	−1.77	1.3105^{-07}
A_15_P108496	*uap1*	UDP-N-acteylglucosamine pyrophosphorylase 1	−1.54	1.1532^{-07}
A_15_P107475	*arl211*	ADP-ribosylation factor-like 2-like 1	−1.46	1.4046^{-07}
A_15_P103005	*mao*	Monoamine oxidase	−1.39	2.1547^{-06}
A_15_P104135	*ndpkz3*	Nucleoside diphosphate kinase-Z3	−1.35	0.00015
A_15_P107149	*ldb3*	LIM-domain binding factor 3	−1.35	1.8293^{-06}
A_15_P105189	*ndpkz3*	Nucleoside diphosphate kinase-Z3	−1.34	0.00015
A_15_P105145	*cnot3a*	CCR4-NOT transcription complex, subunit 3a	−1.31	3.3624^{-07}
A_15_P111655	*ptma*	Prothymosin, alpha	−1.28	1.1762^{-06}

Analysis of *sox11b*, *insm1a*, and c-*myb* Expression in Wild-Type and XOPS-mCFP Zebrafish

Of the genes that displayed increased expression in response to rod degeneration in XOPS-mCFP retinas, several function as transcriptional activators (Supplementary Table S2, http://www.iovs.org/lookup/suppl/doi:10.1167/iovs.10-6022/-/DCSupplemental). We selected three transcription factors, *sox11b*, *insm1a*, and c-*myb*, for further analysis based on their previously described roles in regulating neurogenesis in both the central and peripheral nervous systems.[15–19] We hypothesized that if these genes play a role in regulating regeneration of the rods, we should detect their expression in the ONL where the rod progenitor cells reside. Furthermore, because studies of photoreceptor regeneration in response to acute retinal damage in zebrafish have shown that this process involves reactivation of some developmental signaling pathways,[20–22] we also examined the expression patterns of *sox11b*, *insm1a*, and c-*myb* during retinogenesis by in situ hybridization on retinal sections.

Sex determining region (SRY)-box 11, or Sox11, is a member of the group C family of Sox transcriptional activators. Group C Sox proteins regulate many developmental processes, including heart formation and nervous system development.[23] Zebrafish *sox11b* is one of two co-orthologues of the mammalian *sox11* gene.[24] Expression of *sox11b* has also been reported to increase after light-induced photoreceptor cell death.[25,26] We compared *sox11b* expression patterns in adult wild-type and XOPS-mCFP retinas. In wild-type retinas, *sox11b* expression was observed in the persistently neurogenic ciliary marginal zone (CMZ), but was rarely detected in the central retina (Figs. 4A, 4B). In contrast, in XOPS-mCFP adult retinas, *sox11b* expression was observed in the CMZ and in numerous cells located at the base of the ONL (Figs. 4C, 4D). In the developing wild-type retina at 24 hpf, *sox11b* expression was observed in scattered cells throughout the retinal neuroepithelium and lens (Figs. 4E, 4F). As development proceeded, expression of *sox11b* became restricted to the dorsal and ventral retinal margin (Figs. 4G, 4H). At 48 and 72 hpf, *sox11b* appeared to occupy a larger domain at the dorsal retinal margin compared to the ventral margin. However, in both the dorsal and ventral marginal zones, *sox11b* expression did not extend to the peripheral-most corner of the CMZ.

Insulinoma-associated 1 (insm1) is a zinc-finger transcription factor that is primarily expressed in developing neuroendocrine tissues and in the developing nervous system.[27] Zebrafish *insm1a* is one of two co-orthologues of mammalian *insm1*.[28] *Insm1a* displayed a very similar expression pattern to *sox11b* in both wild-type and XOPS-mCFP adult retinas (Fig. 5). In wild-type adult retina, expression of *insm1a* was detected in only a few cells at the CMZ and was not observed in the central retina (Figs. 5A, 5B). In contrast, in XOPS-mCFP retinas, expression of *insm1a* was detected in both the CMZ and in numerous cells at the base of the ONL where the rod progenitors are located (Figs. 5C, 5D). In XOPS-mCFP retinas, *insm1a* expression was also occasionally observed in the inner nuclear layer (INL) in cells that displayed fingerlike projections suggestive of Müller glia (Fig. 5C), although this has not yet been confirmed by colocalization with a Müller glial marker. Expression of *insm1a* was not detectable in the developing retina at 24 hpf (data not shown). However, by 36 hpf *insm1a* expression was observed throughout the central retinal neuroepithelium (Fig. 5E). Similar to *sox11b*, expression of *insm1a* became restricted to the retinal margins at 48 and 72 hpf, with stronger expression in the dorsal margin compared to the ventral margin (Figs. 5F, 5G).

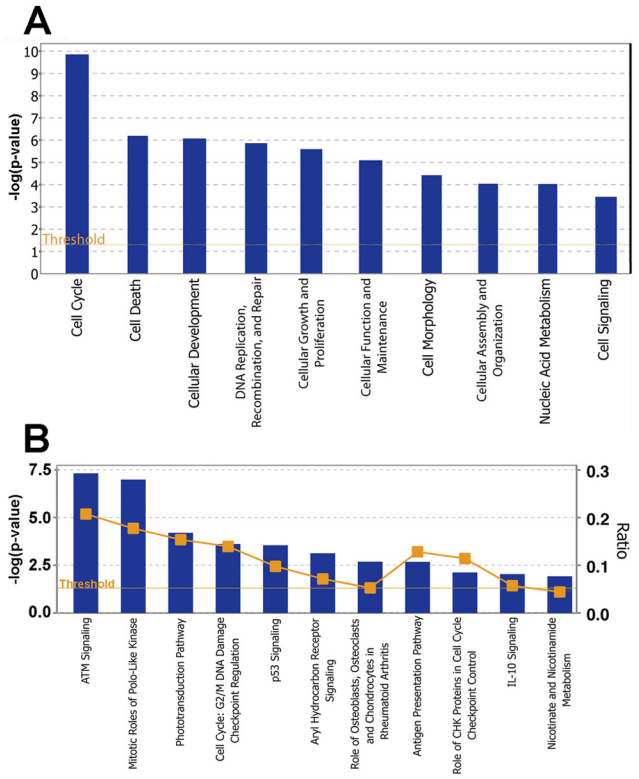

FIGURE 1. Pathway analysis of differentially expressed genes. (**A**) Top ten biological functions associated with gene expression changes between wild-type and XOPS-mCFP retinas. The *y*-axis represents the negative log of the p-value associated with the probability that each biological function was identified due to chance alone. (**B**) Top eleven canonical signaling pathways associated with differentially expressed genes. The blue bars represent the negative log of the p-value associated with the probability that each pathway was identified due to chance alone. The orange squares represent a ratio of the number of molecules from the microarray dataset that were associated with a given canonical pathway divided by the total number of molecules that map to that pathway.

c-Myb is a transcriptional activator best known for its role in regulating hematopoiesis but which has also been recently linked to maintenance of neural stem cells in the brain.[15,29] To study c-*myb* expression, we obtained a transgenic fluorescent reporter line generated in the laboratory of Leonard Zon[10] in which GFP expression is controlled by the c-*myb* promoter. We have shown previously that rod progenitor cell mitotic activity is detectable in wild-type juvenile zebrafish at approximately 10 to 15 dpf.[9] In retinal sections from 16 dpf c-*myb-GFP* transgenic zebrafish, GFP expression was observed in small number of cells located at the base of the ONL where the rod progenitor cells are located (Figs. 6A, 6B). Interestingly, c-*myb* expression was also occasionally observed in isolated Müller glial cells (identified based on their morphology) located in close proximity to the GFP$^+$ ONL cells (Fig. 6A). Because we could not conclusively distinguish between the fluorescent signal from XOPS-mCFP and c-*myb*-GFP expressing cells in XOPS-mCFP animals, we used in situ hybridization analysis to compare c-*myb* expression in adult wild-type and XOPS-mCFP retinas. In wild-type retinal sections from 1-year-old adults, we observed c-*myb* expression mainly in the CMZ (data not shown) and only rarely in the central retina (Fig. 6C), suggesting that the c-*myb*$^+$ ONL cell population is smaller in adult retinas than in juvenile retinas. We did not detect expression of c-*myb* in mature photoreceptors. In age-matched XOPS-mCFP retinal sections, we observed c-*myb* expression in both the CMZ and in a greater number of cells at the base of the ONL than was observed in the wild-type retinas (Fig. 6D), indicating localization of c-*myb* in a subset of ONL cells that likely represent rod progenitor cells or immature rod precursors. However, c-*myb* expression did not appear to be as widespread in the ONL of XOPS-mCFP retinas as *sox11b* or *insm1a*. Expression of c-*myb* was also detected in the INL of XOPS-mCFP retinas (Fig. 6D). The INL c-*myb*+ cells displayed fingerlike projections suggestive of Müller glia, although this remains to be confirmed by co-localization with a Müller glial marker. This expression pattern was rarely observed in wild-type retinas.

During retinal development, expression of endogenous c-*myb* was evident throughout the retinal neuroepithelium at 24 hpf (Fig. 6E). As above, the c-*myb* expression domains became more restricted to the retinal margin as retinogenesis proceeded, and by 72 hpf endogenous c-*myb* expression was confined to the persistently mitotic CMZ (Fig. 6G). In c-*myb-GFP* transgenic zebrafish at 5 dpf, c-*myb-GFP* expression was observed in several Müller glia, as evidenced by the co-localization of GFP with the Müller cell antibody Zrf-1 (Fig. 6H). One possible interpretation of these results is that c-*myb* expression is activated just before cell cycle exit of retinal progenitors fated to become Müller glia.

The expression patterns of *sox11b*, *insm1a*, and c-*myb* at the base of the ONL in adult XOPS-mCFP retinas are consistent with their localization in rod progenitor cells or postmitotic rod precursors. To investigate this further, we performed double in situ hybridizations on cryosections of XOPS-mCFP retinas with DIG-labeled antisense probes for *sox11b*, *insm1a*, or c-*myb*, and a FITC-labeled antisense probe for the cell proliferation marker *PCNA*. We have previously shown that in XOPS-mCFP retinas, rod degeneration results in a significant increase in PCNA$^+$ rod progenitor cells at the base of the ONL.[6,9] In adult XOPS-mCFP retinas, we observed a subset of cells that appeared to be labeled with both the *PCNA* probe and the *sox11b* probe, both in the central retina and in the CMZ (Figs. 7A, 7B). These putative double-positive cells were always adjacent to cells that appeared to label with only the *sox11b* or the *PCNA* probe, but not both. We obtained a very similar labeling pattern for the double in situ hybridization with *insm1a* and *PCNA* probes (Figs. 7C, 7D). One interpretation of these results is that *sox11b* and *insm1a* are expressed in some mitotic rod progenitor cells (perhaps just before cell cycle exit), and that expression is maintained in postmitotic rod precursors. Indeed, we also observed co-localization of *sox11b* and *insm1a* markers in the same cells at the base of the ONL (data not shown), suggesting that these two genes are expressed in the same cell population. When we performed double in situ hybridization with probes for c-*myb* and PCNA we observed what appeared to be extensive co-labeling, both at the margin and in the central retina (Figs. 7E, 7F), which may suggest that in the central retina c-*myb* is expressed primarily in proliferating rod progenitor cells. However, we note that because we used colorimetric assays to detect each probe, which result in a red or purple reaction product that can diffuse away from the cell, we cannot definitively conclude that each probe co-localized with *PCNA* in mitotic rod progenitors. Our results await more definitive classification once antibodies to zebrafish Sox11b, Insm1a, and c-Myb are available.

Taken together, the developmental and adult gene expression patterns of *sox11b*, *insm1a*, and c-*myb* suggest that they play a role in retinal neurogenesis during embryonic development as well as in regulating aspects of the response to rod photoreceptor degeneration.

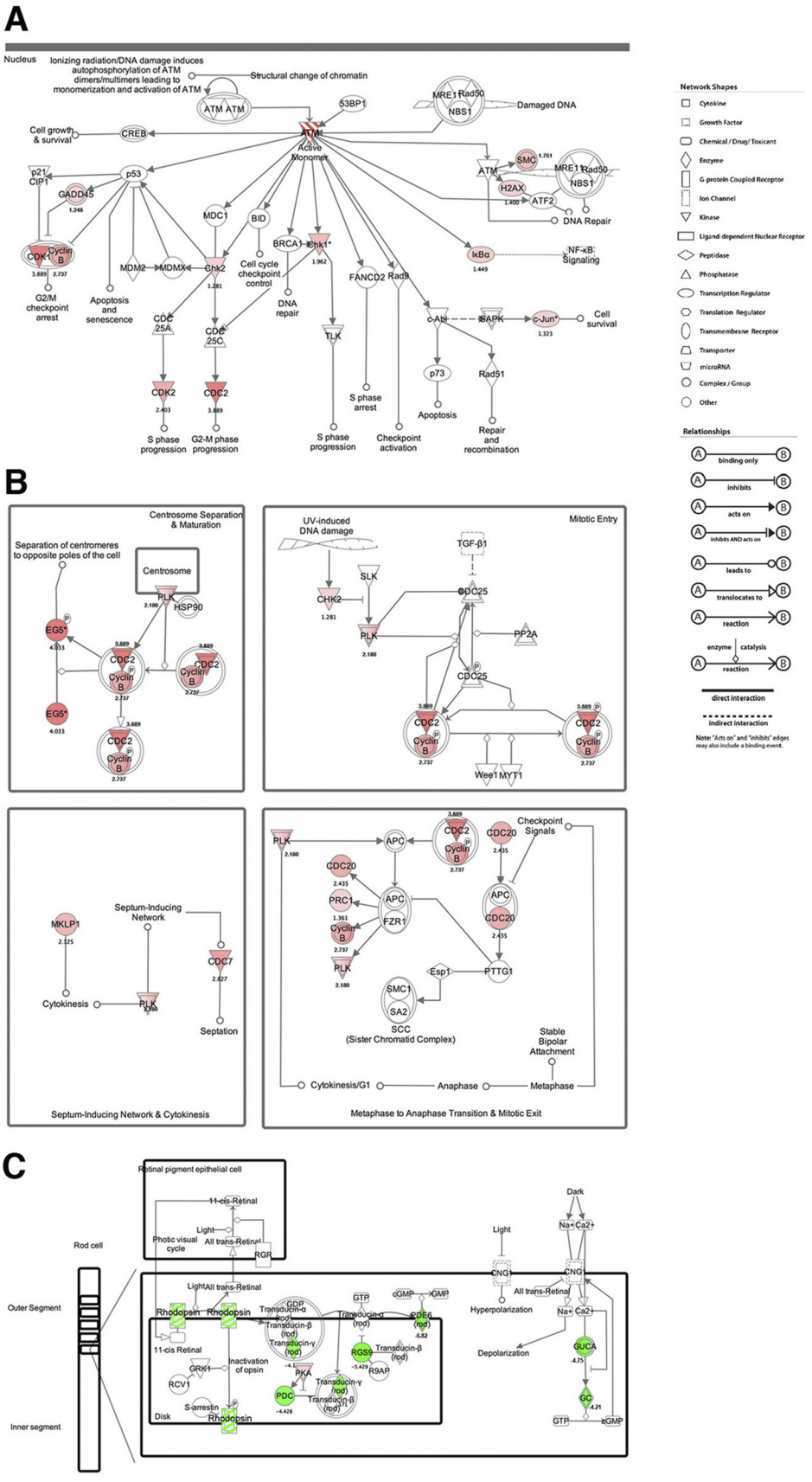

FIGURE 2. Diagrammatic representation of the top three canonical signaling pathways, proposed by the Ingenuity Pathways Analysis program, associated with differentially expressed genes in the microarray dataset. (**A**) The ataxia-telangiectasia mutated (ATM) signaling pathway. (**B**) The mitotic roles of the polo-like kinase (PLK). C) The rod phototransduction pathway. Genes that displayed an increase in expression in XOPS-mCFP retinas compared to wild-type are shaded in red; genes that displayed a decrease in expression are shaded in green. The hatched shading for ATM (**A**) and rhodopsin (**C**) indicates their manual annotation in the pathways. A legend describing the symbols used in each pathway is shown in the upper right portion of the figure.

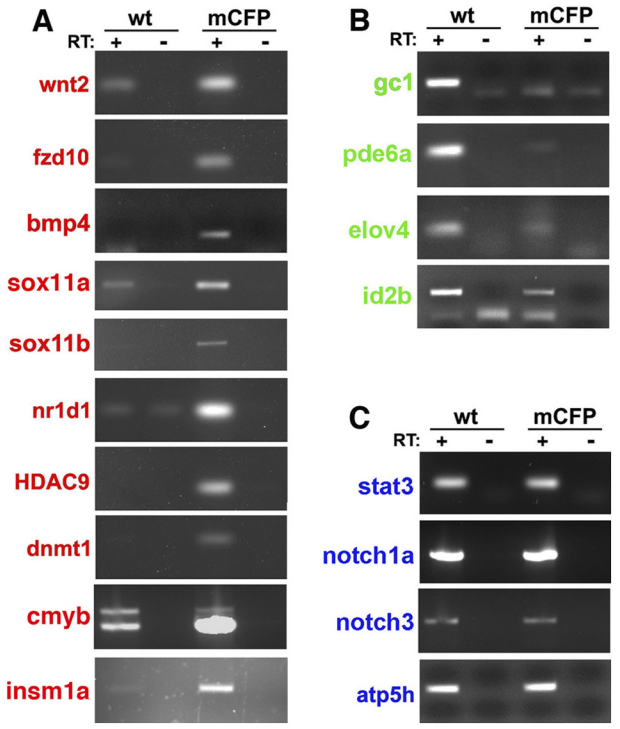

Figure 3. RT-PCR analysis for selected genes to confirm the microarray results. (**A**) Genes that display an increase in expression in XOPS-mCFP (mCFP) retinas compared to wild-type (wt). (**B**) Genes that display a decrease in expression. (**C**) Genes that show no change in expression between XOPS-mCFP and wild-type retinas. RT, reverse transcriptase.

Discussion

In the present study, we used microarray analysis to determine the retinal gene expression profile of XOPS-mCFP transgenic zebrafish, in which a continual cycle of rod photoreceptor death and regeneration results in a chronically elevated population of rod progenitor cells. Our study is distinct from other recent microarray analyses of intact and regenerating zebrafish retinas,[25,26,30,31] because we have made use of a genetic model that experiences selective, chronic rod photoreceptor degeneration, rather than acute loss of both rods and cones or other retinal neurons. As such, the gene expression changes we observed were less likely to be associated with processes such as clearance of cellular debris and wound healing, and more likely to be related directly to rod photoreceptor degeneration and regeneration. Furthermore, we have shown previously that chronic degeneration of rods does not induce proliferation of Müller glia in zebrafish,[6,9] whereas others have shown that photoreceptor regeneration after acute retinal damage is dependent on the Müller glial response.[21,30,32,33] Therefore, it is not surprising that the genes identified in our microarray analysis constitute a distinct, yet overlapping, set of genes from those associated with regeneration in the acutely damaged zebrafish retina. For example, genes associated with cell proliferation (such as *mps1*, the cyclins, and the *mcms*), and transcriptional regulation (such as *sox11b*, *her9*, *id2b*, *olig2*, and *ascl1a*, among others) displayed expression changes in XOPS-mCFP retinas similar to what has been observed in response to acute retinal damage (Supplementary Tables S1, S2, http://www.iovs.org/lookup/suppl/doi:10.1167/iovs.10-6022/-/DCSupplemental). In contrast, genes such as *stat3*, *hspd1*, *pax6a*, *pax6b*, *mdka*, *mdkb*, and *gal-l2*, which display increased expression in response to acute photoreceptor cell death,[21,26,30,33,34] did not change in expression in response to selective rod degeneration. These results suggest that our approach, in combination with the data from other groups studying acute retinal damage in zebrafish, may allow us to better define the

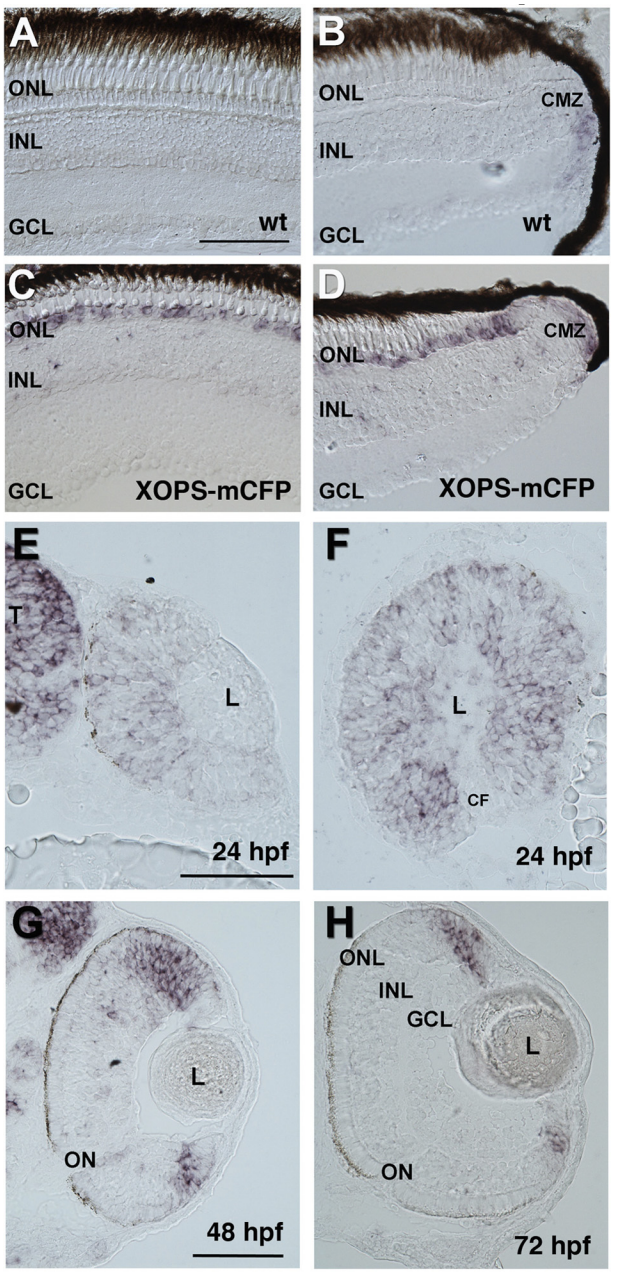

Figure 4. *Sox11b* expression in wild-type and XOPS-mCFP retinas. In situ hybridization with an antisense probe for *sox11b* was performed on cryosections of adult wild-type retina (**A**, **B**), adult XOPS-mCFP retina (**C**, **D**), and developing wild-type retina (**E**–**H**). *Sox11b* expression was not detected in wild-type central retina (**A**) and was present at the ciliary marginal zone (CMZ) of wild-type peripheral retina (**B**). In contrast, *sox11b* was strongly expressed in cells at the base of the outer nuclear layer (ONL) in XOPS-mCFP central (**C**) and peripheral (**D**) retina. Transverse (**E**) and sagittal (**F**) sections through the developing retina at 24 hpf show scattered expression of *sox11b*. By 48 hpf (G) *sox11b* expression was restricted to the retinal margin, and was observed only in the CMZ at 72 hpf (**H**). (**E**–**H**) Dorsal is toward the top of the image. GCL, ganglion cell layer; INL, inner nuclear layer; ONL, outer nuclear layer; L, lens; T, telencephalon; CF, choroid fissure; ON, optic nerve. Scale bar: 50 μm.

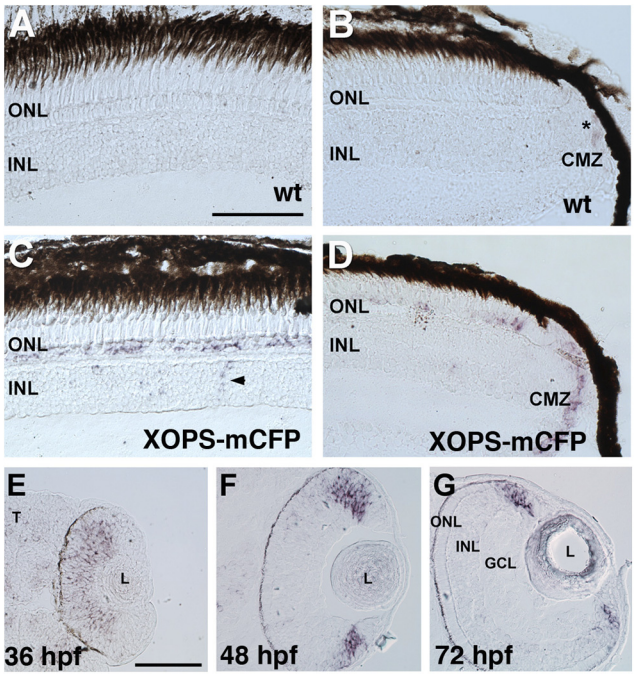

FIGURE 5. *Insm1a* expression in wild-type and XOPS-mCFP retinas. In situ hybridization with an antisense probe for *insm1a* was performed on cryosections of adult wild-type retina (**A**, **B**), adult XOPS-mCFP retina (**C**, **D**), and developing wild-type retina (**E**–**G**). *Insm1a* expression was not detected in wild-type central retina (**A**) and was present in a few cells at the ciliary marginal zone (CMZ, asterisk) of wild-type peripheral retina (**B**). In XOPS-mCFP retinas, *insm1a* was expressed in numerous cells at the base of the outer nuclear layer (ONL) and occasionally in cells of the inner nuclear layer (INL) that had a Müller glia morphology (**C**, *arrowhead*). *Insm1a* was observed in the central developing retina at 36 (**E**). By 48 hpf (**F**) *insm1a* expression was restricted to the retinal margin, and was observed only in the CMZ at 72 hpf (**G**). (**E**–**G**) Dorsal is toward the top of the image. CMZ, ciliary marginal zone; INL, inner nuclear layer; ONL, outer nuclear layer; L, lens; T, telencephalon. Scale bar: 50 μm.

genetic pathways that mediate the response to chronic versus acute photoreceptor cell loss.

We made use of a pathway analysis database (Ingenuity Systems) to visualize the set of enriched gene groups in a network format. One of the top canonical pathways that were identified by the IPA analysis is the ATM signaling pathway. This pathway is triggered by DNA damage, which in turn activates the ataxia telangiectasia mutated (ATM) protein kinase. Activation of ATM signaling results in several downstream events, including initiation of DNA repair, activation of cell cycle checkpoints, and apoptosis.[35] It has been shown in animal and in vitro models of retinitis pigmentosa that photoreceptor degeneration is correlated with both an increase in reactive oxygen species (ROS) and an increase in oxidative DNA damage.[36–39] Therefore, it is possible that the toxic effects of the XOPS-mCFP transgene result in a similar increase in ROS and DNA damage, leading to activation of the ATM pathway and apoptosis. Alternatively, increased expression of genes in the ATM pathway may be more closely related to regeneration than to cell death. Intriguingly, a recent study of the MRL healer mouse, which displays unique regenerative and wound-healing abilities not normally observed in mammals, revealed that this strain exhibits a cell cycle checkpoint defect, reduced p21 expression, enhanced G_2/M arrest, and an increase in DNA damage,[40] suggesting an association between the DNA damage response and regenerative ability.

The mitotic roles of the polo-like kinase (PLK) represent another canonical pathway displaying significant association with differentially expressed genes in our microarray dataset. PLK is a highly conserved protein that regulates entry of cells into the M phase.[41] The increase in expression of *plk1*, as well as genes coding for its cell cycle-related targets, in our microarray dataset likely reflects the increase in proliferation of rod progenitor cells in response to rod degeneration.

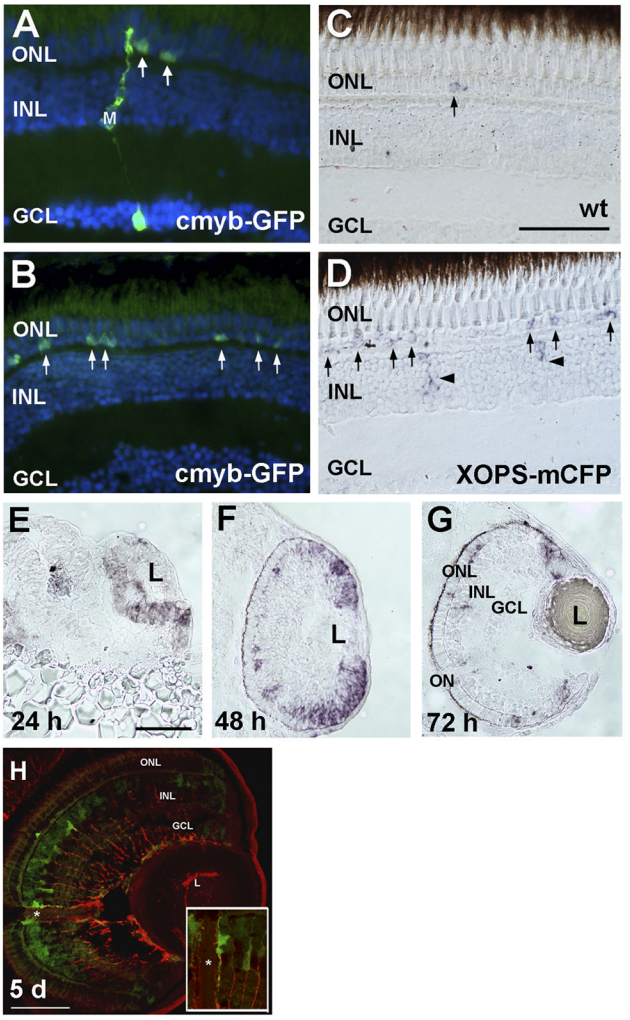

FIGURE 6. c-myb and c-*myb-GFP* expression in wild-type and XOPS-mCFP retinas. (**A**, **B**) GFP fluorescence in retinal cryosections from 16 dpf *cmyb-GFP* animals. Nuclei were stained with DAPI (*blue*). GFP expression was detectable in rod progenitor cells in the outer nuclear layer (**A**, **B**, *arrows*) and in rare Müller glia (**B**). (**C**, **D**) In situ hybridization of adult wild-type (**C**) and XOPS-mCFP (**D**) cryosections with c-*myb* antisense probe. C-*myb* expression was rarely detected in wild-type retina (**C**, *arrow*) but was increased in the outer nuclear layer of XOPS-mCFP retina (**D**, *arrows*). C-*myb* expression was also observed cells resembling Müller glia (**D**, *arrowheads*) in the XOPS-mCFP retina. (**E**–**G**) In situ hybridization of cryosections through the wild-type developing retina. Dorsal is toward the top of the image. Developmental stages for (**A**) and (**B**) are indicated at the bottom of the panels. Expression of c-*myb* was progressively restricted to the CMZ as development proceeded. (**H**) Immunolabeling of 5 dpf c-*myb-GFP* retinal cryosection with Zrf-1, which labels Müller glia (*red*). Inset shows higher magnification of the region near the optic nerve (asterisk). GFP expression (*green*) colocalized with Müller glia immunoreactivity at this stage. GCL, ganglion cell layer; INL, inner nuclear layer; ONL, outer nuclear layer; CMZ, ciliary marginal zone; L, lens; ON, optic nerve. Scale bar: 50 μm.

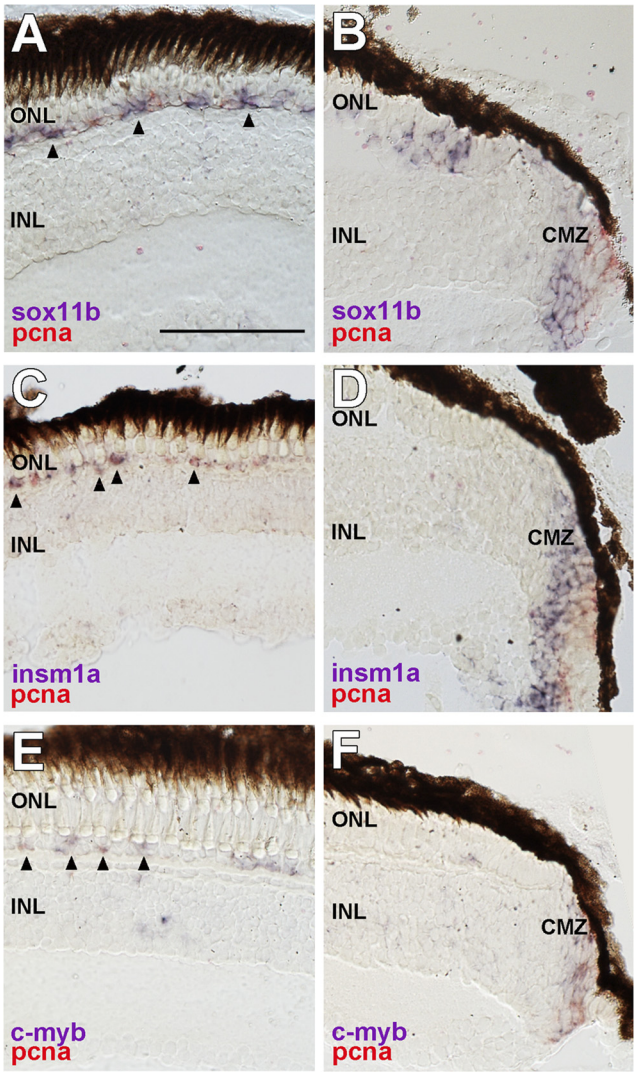

FIGURE 7. Expression of *sox11b*, *insm1a*, c-*myb*, and *PCNA* in XOPS-mCFP retinas. In situ hybridization with DIG-labeled antisense probes for *sox11b* (**A**, **B**), *insm1a* (**C**, **D**), and c-*myb* (**E**, **F**) and a FITC-labeled probe for *PCNA* (**A**–**F**) was performed on cryosections of adult XOPS-mCFP retinas. Labeled cells in the central retina are shown in (**A**), (**C**), and (**E**). Expression at the retinal margin is shown in (**B**), (**D**), and (**F**). *Black arrowheads*: cells that appear to double-label with *PCNA* and *sox11b* (**A**), *insm1a* (**C**), or c-*myb* (**E**). GCL, ganglion cell layer; INL, inner nuclear layer; ONL, outer nuclear layer; CMZ, ciliary marginal zone. Scale bar: 50 μm.

The IPA program also identified a significant correlation between differentially expressed genes in our dataset and the rod phototransduction pathway. This result is not surprising, because mature rod photoreceptors degenerate in XOPS-mCFP retinas because of the toxic effects of the XOPS-mCFP transgene, and it confirms the accuracy and sensitivity of the IPA analysis.

Because we are interested in identifying the transcriptional regulatory networks that regulate photoreceptor regeneration in zebrafish, we chose to study further three transcription factors, with previously described roles in neurogenesis, that demonstrated increased expression in XOPS-mCFP retinas. These include the zebrafish homologues of *insm1*, a zinc-finger transcription factor associated with neuroendocrine development and neurogenesis[27,42]; *sox11*, a transcription factor involved in the regulation of embryonic development and neural cell fate determination[19,23]; and c-*myb*, a transcription factor best known for its role in regulating hematopoiesis but which has also been linked to maintenance of neural stem cells.[15] In situ hybridization analysis demonstrated that in wild-type zebrafish all three genes are expressed in the CMZ, suggesting that they are involved in persistent neurogenesis in the adult retina. Furthermore, expression of all three genes was localized to the base of the ONL in the XOPS-mCFP retinas, where mitotic rod progenitor cells and postmitotic rod precursors have been shown to reside.[6,9] Double in situ hybridization analysis indicated that some *sox11b*$^+$, *insm1a*$^+$, and c-*myb*$^+$ cells co-localized with the proliferation marker PCNA, although this result is not conclusive because of the technical limitations of the colorimetric in situ assay. In single in situ hybridization experiments, *sox11b* and *insm1a* demonstrated the most widespread expression in the ONL of XOPS-mCFP retinas. This may suggest that they are expressed in both mitotic and postmitotic rod progenitors. Indeed, previous studies have suggested a role for *insm1* and *sox11* in regulating progenitor cell cycle exit and the establishment of neuronal identity, respectively[43–45]; therefore, it is possible that they act in a similar fashion to regulate rod photoreceptor regeneration. Interestingly, both c-*myb* and to some extent *insm1a* displayed an increase in expression in cells that had a Müller glial morphology in XOPS-mCFP retinas. At this point the functional significance of this expression pattern is unclear and must be confirmed using Müller-glial–specific markers in adult retinal sections (although we did observe co-localization of c-*myb*-GFP with the Müller glial antibody Zrf-1 at 5 dpf). We have demonstrated that Müller glia do not proliferate or show signs of reactive gliosis in XOPS-mCFP retinas.[6,9] The increase in expression of c-*myb* and *insm1a* in a subset of Müller glia may be associated with a proliferation-independent signaling pathway in response to chronic rod degeneration. Alternatively, we cannot rule out the possibility that c-*myb* and *insm1a* are expressed in a subset of Müller glia proliferating at a much slower rate than is observed in response to acute retinal damage, below the threshold of detection in our assays.

Our in situ hybridization expression data also support a role for *sox11b*, *insm1a*, and c-*myb* during retinal development. Although the developmental stage at which expression of each gene was first detected differed somewhat (24 hpf for *sox11b* and c-*myb*, 36 hpf for *insm1a*) the general expression patterns throughout retinal development were similar for all three genes. As retinal development proceeded, expression of all three genes became progressively restricted to the proliferative retinal margin, indicating that these genes are not expressed in differentiated retinal neurons, but rather may function at the stage of retinal progenitor proliferation, specification, or exit from the cell cycle. Interestingly, in contrast to the c-*myb* expression pattern visualized by in situ hybridization, in the c-*myb*-GFP transgenic line, GFP expression persisted in the central retina through 5 dpf and was colocalized with the Müller cell marker Zrf-1. This may indicate that c-*myb* expression is activated just before cell cycle exit in progenitor cells fated to become Müller glia (and the stable expression of GFP marks these cells even after expression of endogenous c-*myb* has been terminated). Furthermore, the close association of GFP$^+$ rod progenitor cells and isolated GFP$^+$ Müller glia in juvenile c-*myb-GFP* retinas suggests that c-*myb* may be a marker for the stem-cell–producing subset of Müller glia.

In summary, our results provide new information regarding the molecular determinants of the response to rod photoreceptor degeneration in zebrafish and identify novel transcriptional regulators of both rod photoreceptor regeneration and retinal development. Although the roles of *sox11*, *insm1*, and c-*myb* in retinal development have not been directly tested in higher vertebrates, they have all been shown to be expressed in the developing mammalian retina.[16,46,47] Thus, further ex-

amination of the role of these genes in regulating photoreceptor development and regeneration in zebrafish may be relevant to mammalian photoreceptor development as well.

Acknowledgments

The authors thank Katherine Lewis Loughlin, Anthony Roberts, and Gina Rockholt Johnson for animal care, and the staff of the Biological Science Imaging Resources Facility at Florida State University.

References

1. Morris AC, Fadool JM. Studying rod photoreceptor development in zebrafish. *Physiol Behav.* 2005;86:306–313.
2. Fadool JM, Dowling JE. Zebrafish: A model system for the study of eye genetics. *Prog Retin Eye Res.* 2008;27:89–110.
3. Schmitt EA, Dowling JE. Early retinal development in the zebrafish, danio rerio: Light and electron microscopic analyses. *J Comp Neurol.* 1999;404:515–536.
4. Easter SS, Jr., Nicola GN. The development of vision in the zebrafish (danio rerio). *Dev Biol.* 1996;180:646–663.
5. Hitchcock P, Ochocinska M, Sieh A, Otteson D. Persistent and injury-induced neurogenesis in the vertebrate retina. *Prog Retin Eye Res.* 2004;23:183–194.
6. Morris AC, Schroeter EH, Bilotta J, Wong RO, Fadool JM. Cone survival despite rod degeneration in XOPS-mCFP transgenic zebrafish. *Invest Ophthalmol Vis Sci.* 2005;46:4762–4771.
7. Otteson DC, Hitchcock PF. Stem cells in the teleost retina: persistent neurogenesis and injury-induced regeneration. *Vision Res.* 2003;43:927–936.
8. Westerfield M. *The Zebrafish Book: A Guide for the Laboratory Use of Zebrafish* (*brachydanio rerio*). Eugene, OR: University of Oregon Press; 1995.
9. Morris AC, Scholz TL, Brockerhoff SE, Fadool JM. Genetic dissection reveals two separate pathways for rod and cone regeneration in the teleost retina. *Dev Neurobiol.* 2008;68:605–619.
10. North TE, Goessling W, Walkley CR, et al. Prostaglandin E2 regulates vertebrate haematopoietic stem cell homeostasis. *Nature.* 2007;447:1007–1011.
11. Bertrand JY, Kim AD, Teng S, Traver D. CD41+ cmyb+ precursors colonize the zebrafish pronephros by a novel migration route to initiate adult hematopoiesis. *Development.* 2008;135:1853–1862.
12. Benjamini Y, Hochberg Y. Controlling the false discovery rate: A practical and powerful approach to multiple testing. *J Royal Stat Soc B.* 1995;57:289.
13. Edgar R, Domrachev M, Lash AE. Gene expression omnibus: NCBI gene expression and hybridization array data repository. *Nucleic Acids Res.* 2002;30:207–210.
14. Ceresa M, Masseroli M, Campi A. A web-enabled database of human gene expression controlled annotations for gene list functional evaluation. *Conf Proc IEEE Eng Med Biol Soc.* 2007; 2007:394–397.
15. Malaterre J, Mantamadiotis T, Dworkin S, et al. c-myb is required for neural progenitor cell proliferation and maintenance of the neural stem cell niche in adult brain. *Stem Cells.* 2008;26:173–181.
16. Duggan A, Madathany T, de Castro SC, Gerrelli D, Guddati K, Garcia-Anoveros J. Transient expression of the conserved zinc finger gene INSM1 in progenitors and nascent neurons throughout embryonic and adult neurogenesis. *J Comp Neurol.* 2008; 507:1497–1520.
17. Breslin MB, Zhu M, Lan MS. NeuroD1/E47 regulates the E-box element of a novel zinc finger transcription factor, IA-1, in developing nervous system. *J Biol Chem.* 2003;278:38991–38997.
18. Jankowski MP, McIlwrath SL, Jing X, et al. Sox11 transcription factor modulates peripheral nerve regeneration in adult mice. *Brain Res.* 2009;1256:43–54.
19. Haslinger A, Schwarz TJ, Covic M, Chichung Lie D. Expression of Sox11 in adult neurogenic niches suggests a stage-specific role in adult neurogenesis. *Eur J Neurosci.* 2009;29:2103–2114.
20. Raymond PA, Barthel LK, Bernardos RL, Perkowski JJ. Molecular characterization of retinal stem cells and their niches in adult zebrafish. *BMC Dev Biol.* 2006;6:36.
21. Thummel R, Enright JM, Kassen SC, Montgomery JE, Bailey TJ, Hyde DR. Pax6a and Pax6b are required at different points in neuronal progenitor cell proliferation during zebrafish photoreceptor regeneration. *Exp Eye Res.* 2010;90:572–582.
22. Yurco P, Cameron DA. Cellular correlates of proneural and notch-delta gene expression in the regenerating zebrafish retina. *Vis Neurosci.* 2007;24:437–443.
23. Penzo-Mendez AI. Critical roles for SoxC transcription factors in development and cancer. *Int J Biochem Cell Biol.* 2010;42:425–428.
24. Navratilova P, Fredman D, Lenhard B, Becker TS. Regulatory divergence of the duplicated chromosomal loci sox11a/b by subpartitioning and sequence evolution of enhancers in zebrafish. *Mol Genet Genomics.* 2010;283:171–184.
25. Craig SE, Calinescu AA, Hitchcock PF. Identification of the molecular signatures integral to regenerating photoreceptors in the retina of the zebra fish. *J Ocul Biol Dis Infor.* 2008;1:73–84.
26. Kassen SC, Ramanan V, Montgomery JE, et al. Time course analysis of gene expression during light-induced photoreceptor cell death and regeneration in albino zebrafish. *Dev Neurobiol.* 2007;67:1009–1031.
27. Lan MS, Breslin MB. Structure, expression, and biological function of INSM1 transcription factor in neuroendocrine differentiation. *FASEB J.* 2009;23:2024–2033.
28. Lukowski CM, Ritzel RG, Waskiewicz AJ. Expression of two insm1-like genes in the developing zebrafish nervous system. *Gene Expr Patterns.* 2006;6:711–718.
29. Oh IH, Reddy EP. The myb gene family in cell growth, differentiation and apoptosis. *Oncogene.* 1999;18:3017–3033.
30. Qin Z, Barthel LK, Raymond PA. Genetic evidence for shared mechanisms of epimorphic regeneration in zebrafish. *Proc Natl Acad Sci USA.* 2009;106:9310–9315.
31. Cameron DA, Gentile KL, Middleton FA, Yurco P. Gene expression profiles of intact and regenerating zebrafish retina. *Mol Vis.* 2005; 20:775–791.
32. Thummel R, Kassen SC, Montgomery JE, Enright JM, Hyde DR. Inhibition of muller glial cell division blocks regeneration of the light-damaged zebrafish retina. *Dev Neurobiol.* 2008;68:392–408.
33. Craig SE, Thummel R, Ahmed H, Vasta GR, Hyde D, Hitchcock PF. The zebrafish galectin Drgal1–L2 is expressed by proliferating muller glia and photoreceptor progenitors and regulates the regeneration of rod photoreceptors. *Invest Ophthalmol Vis Sci.* 2010;51:3244–3252.
34. Calinescu AA, Vihtelic TS, Hyde DR, Hitchcock PF. Cellular expression of midkine-a and midkine-b during retinal development and photoreceptor regeneration in zebrafish. *J Comp Neurol.* 2009;514:1–10.
35. Lavin MF. Ataxia-telangiectasia: From a rare disorder to a paradigm for cell signalling and cancer. *Nat Rev Mol Cell Biol.* 2008;9:759–769.
36. Carmody RJ, McGowan AJ, Cotter TG. Reactive oxygen species as mediators of photoreceptor apoptosis in vitro. *Exp Cell Res.* 1999; 248:520–530.
37. Sharma AK, Rohrer B. Sustained elevation of intracellular cGMP causes oxidative stress triggering calpain-mediated apoptosis in photoreceptor degeneration. *Curr Eye Res.* 2007;32:259–269.
38. Doonan F, Donovan M, Cotter TG. Activation of multiple pathways during photoreceptor apoptosis in the rd mouse. *Invest Ophthalmol Vis Sci.* 2005;46:3530–3538.
39. Sanz MM, Johnson LE, Ahuja S, Ekstrom PA, Romero J, van Veen T. Significant photoreceptor rescue by treatment with a combination of antioxidants in an animal model for retinal degeneration. *Neuroscience.* 2007;145:1120–1129.
40. Bedelbaeva K, Snyder A, Gourevitch D, et al. Lack of p21 expression links cell cycle control and appendage regeneration in mice. *Proc Natl Acad Sci USA.* 2010;107:5845–5850.
41. Archambault V, Glover DM. Polo-like kinases: Conservation and divergence in their functions and regulation. *Nat Rev Mol Cell Biol.* 2009;10:265–275.
42. Farkas LM, Haffner C, Giger T, et al. Insulinoma-associated 1 has a panneurogenic role and promotes the generation and expansion

of basal progenitors in the developing mouse neocortex. *Neuron.* 2008;60:40–55.

43. Jacob J, Storm R, Castro DS, et al. Insm1 (IA-1) is an essential component of the regulatory network that specifies monoaminergic neuronal phenotypes in the vertebrate hindbrain. *Development.* 2009;136:2477–2485.
44. Zhang T, Liu WD, Saunee NA, Breslin MB, Lan MS. Zinc finger transcription factor INSM1 interrupts cyclin D1 and CDK4 binding and induces cell cycle arrest. *J Biol Chem.* 2009;284:5574–5581.
45. Bergsland M, Werme M, Malewicz M, Perlmann T, Muhr J. The establishment of neuronal properties is controlled by Sox4 and Sox11. *Genes Dev.* 2006;20:3475–3486.
46. Sitzmann J, Noben-Trauth K, Klempnauer KH. Expression of mouse c-myb during embryonic development. *Oncogene.* 1995; 11:2273–2279.
47. Wurm A, Sock E, Fuchshofer R, Wegner M, Tamm ER. Anterior segment dysgenesis in the eyes of mice deficient for the high-mobility-group transcription factor Sox11. *Exp Eye Res.* 2008; 86:895–907.